Mean Horizontal Wind in an Inversion-Capped Convective Boundary Layer

CLAUDE KLAPISZ AND ALAIN WEILL

Centre de Recherches en Physique de l'Environnement (Centre National d'Etudes des Télécommunications/Centre National de la Recherche Scientifique), 92131 Issy-Les-Moulineaux, France

(Manuscript received 19 June 1981, in final form 14 January 1982)

ABSTRACT

We have studied a set of detailed mean horizontal wind profiles obtained with a three-component Doppler sodar. For inversion-capped, convective boundary layer conditions, empirical expressions for the mean horizontal wind and the wind shear in the first few hundred meters of the atmosphere are presented. The observations are parameterized with the height of the lowest inversion z_i, the Monin-Obukhov length L and the friction velocity u_*. From experimental values and empirical expressions, values for the turbulent heat flux are then deduced.

1. Introduction

The evolution of the planetary boundary layer (PBL) capped by a temperature inversion is now reasonably documented and understood (Tennekes, 1973a; Stull, 1976; Kaimal *et al.*, 1976; Caughey and Kaimal, 1977; Deardorff, 1979; Dubosclard, 1980; Artaz and André, 1980). However, one still unsolved problem is the parameterization of the vertical momentum flux and the mean horizontal wind. These quantities are important to the dynamics of the inversion rise as both quantities appear in the turbulent kinetic energy budget.

A number of numerical models of the PBL evolution developed in recent years successfully reproduced most of the meteorological processes observed both during the Wangara (Deardorff, 1974; Wyngaard and Coté, 1974; Pielke and Mahrer, 1975; Zeman and Lumley, 1976; André *et al.*, 1978) and Minnesota experiments (Kaimal *et al.*, 1976). One of the areas in which contemporary models have difficulty is the prediction of the mean horizontal wind, particularly in the convective boundary layer. This has been attributed to the effects of advection, turbulence and local pressure gradient forces. This paper presents a set of detailed mean horizontal wind profiles in the convective boundary layer. The profiles were measured with a three-component Doppler sodar in well-defined meteorological conditions. The detailed sodar measurements allow both fine spatial resolution (one data point every 15 m) and for practical purposes, temporal continuity.

The governing parameters of the turbulent regime in a barotropic unstable PBL are the surface friction velocity u_*, the Monin-Obukhov length L, the Coriolis parameter f, and the depth h of the PBL (Zilitinkevich and Deardorff, 1974). The height h corresponds to the height where the sensible heat flux vanishes at the beginning of the free atmosphere. In the early morning, the inversion base height z_i corresponding to a negative and minimum heat flux is much smaller than h and, consequently, it may be assumed that the Coriolis force has negligible effect on the convective boundary layer. This situation thus offers the possibility of studying a simplified system and to verify the validity of using a limited set of governing parameters (u_*, L, z_i) in the convective layer.

First, we describe the meteorological conditions during the experiment, and the data reduction procedures. Next, we give observations drawn from the study of more than 20 mean horizontal wind profiles in the convective boundary layer. Then an attempt to parameterize the nondimensionalized vertical shear of the horizontal wind and the mean horizontal wind is presented and the validity of our representation through systematic comparisons with sodar measurements as well as tower measurements is assessed. Finally, we also verify the empirical relation using some results from the Wangara campaign. In this case, z_i is $\sim$1000 m but since we are in the presence of a well-mixed layer without wind shear and with a non-negligible wind shear in the inversion layer, we can use the same relation as before.

2. Experimental details

a. Experimental site and instrumentation

The experiments described in this paper were performed during the month of July 1977 at the experimental site of Voves-Villeau, 100 km south of Paris. The site is located within the very flat region of "Beauce".

A number of scientists participated in the coop-

0021-8952/82/050648-08$06.00

erative experiment which yielded a variety of meteorological data. Besides the CRPE three-component Doppler sodar, which has been extensively described in the literature (Aubry *et al.*, 1974; Weill *et al.*, 1978), there were two meteorological towers, 12 and 30 m high, equipped with temperature probes and anemometers. An energy balance measuring device (Perrier *et al.*, 1976) was operated by a group of agricultural meteorologists from the Institut National de Recherche Agronomique (INRA) and rawinsondes were launched regularly by the Etablissement d'Études et de Recherches Météorologiques (EERM) providing humidity and potential temperature profiles every 2 h.

b. *Situations investigated*

In order to improve our understanding of the mechanisms involved in the inversion rise, our work was focused on the early morning evolution of the convective layer of the PBL. Two mornings, for which we had a complete set of measurements were examined in particular.

On both days, the atmosphere was clear, dry and cloudless. On 2 July, the friction velocity was ~0.5 m s^{-1} and the inversion base at 0700 (all times LT) ~200 m. On 6 July, the friction velocity was significantly lower at ~0.3 m s^{-1} and the inversion base at 0700 was ~100 m. The surface heat flux evolution for each day is shown in Fig. 1. It is seen that the radiative heat flux is a maximum at 1200 both days; thus, the maxima of the sensible heat flux which is a part of the radiative heat flux occurs at different times and the flux is much weaker the second day.

Both days were convective situations, with ascending thermals in the lower atmosphere and a well-defined inversion base.

c. *Data treatment*

The backscattered acoustic intensity, proportional to the temperature structure function, commonly termed "reflectivity," is received by each sodar antenna. It is recorded as a function of time and height in tables of 1300 × 30 matrix (30 gates with a spacing of 17 m and 1300 shots with a spacing of 4 s). A backward-forward method is used to find the maximum and the minimum of reflectivity. Since we are only interested here in the maximum of reflectivity, the height x of which is evident on each shot, unnecessary data were eliminated. As the evolution of this height is disturbed by turbulence and oscillation, we choose to follow its secular rise as established using a low-pass filter (Alavi and Jenkins, 1965). With this filter, the averaged height for the maximum of reflectivity is

$$z_i(t) = \sum_{n=-N}^{n=N} A_n x(t + n\Delta t), \qquad (1)$$

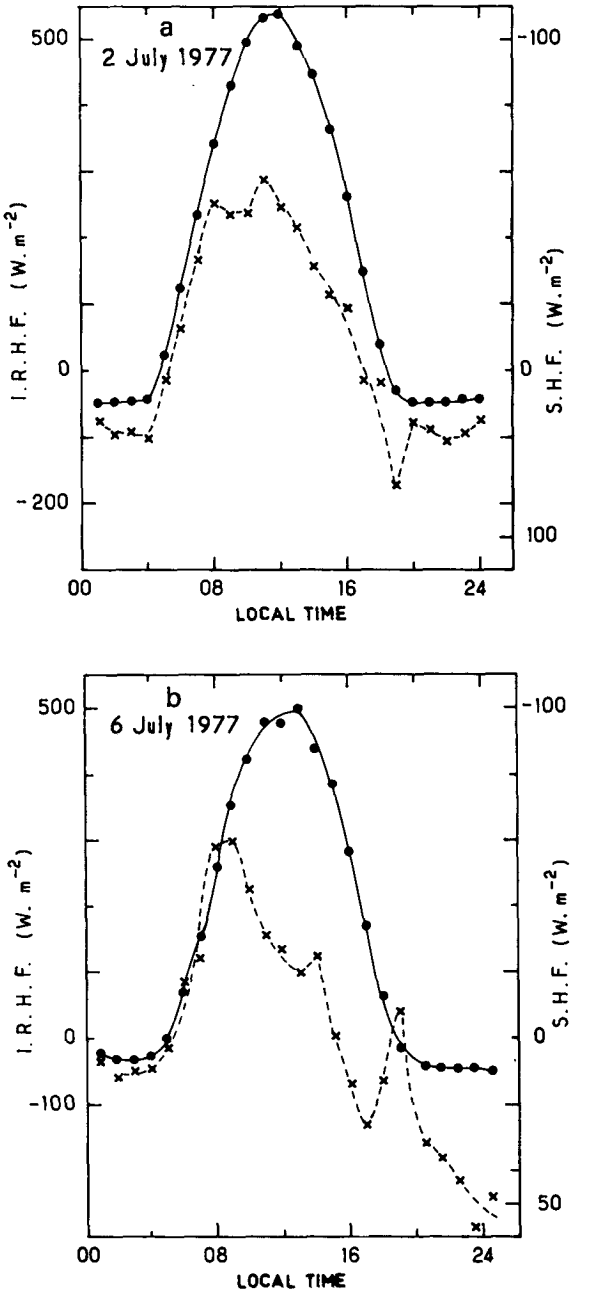

FIG. 1. Incident radiative heat flux (solid line) and sensible heat flux (dashed and crossed line) as measured by the energy balance method of Perrier *et al.* (1976) for 2 July 1977(a) and 6 July 1977(b). (Notice the different scales.)

with the filter coefficient

$$A_n = \frac{1}{2(N+1)}\left(1 + \cos\frac{n\pi}{N+1}\right).$$

This filter has the advantage of having the transfer function $k(f) \to 1$ as frequency $f \to 0$, but the disadvantage of having a cut-off frequency which is not drastically clean.

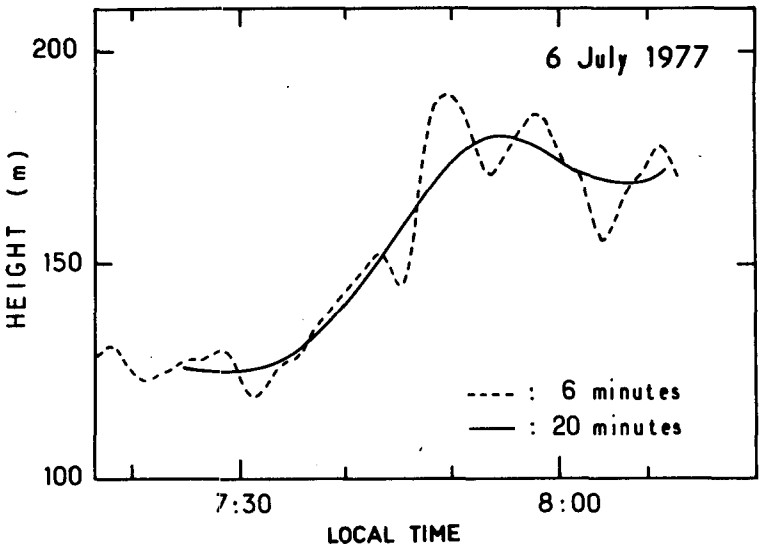

FIG. 2. The height of maximum reflectivity obtained using two different averaging periods.

The evolution of the reflectivity maximum height obtained with the vertical antenna is shown in Fig. 2 for two different averaging times. This method is described in Bouteloup (1981). It can be seen that high-frequency variations are eliminated and that the long-term behavior is retained. An averaging period of 20 min has been used throughout this study. It appears to be adequate to study inversion rise in connection with conventional heat flux measurement, although important information with respect to entrainment is eliminated as the results of individual thermals which appear in 6 min data.

The Doppler data were similarly processed and the horizontal wind velocities were obtained using the same 20 min averaging and filtering process. Table 1 shows the very good agreement between the values thus obtained with the sodar and with the 30 m tower.

TABLE 1. Horizontal wind velocity (m s^{-1}) estimates: a comparison. Voves, 2 July 1977.

Local time	Sodar estimate second gate (19–34 m)	Tower estimate 22 m	Tower estimate 30 m
0555	3.5	3.5	3.9
0605	3.7	3.4	3.8
0615	4.1	3.8	4.2
0625	4.4	4.5	4.9
0635	4.7	4.4	4.8
0645	4.8	4.8	4.8
0715	5.6	5.5	5.5
0725	5.6	5.5	5.8
0735	5.6	5.4	5.8
0745	5.6	5.4	5.9
0755	4.8	4.7	4.9

3. The mean horizontal wind in the convective boundary layer

The friction velocity u_* and the Monin-Obukhov length L were derived from the 12 and 30 m tower measurements; the best set of parameters was found from wind-speed values in the surface layer using the Paulson expression (see Section 4). The kinematic heat flux was also determined at a height of 2 m by the balance method of Perrier *et al.* (1976). With the sodar, we are able to follow continuously the convective layer top z_i, which can be identified with the height of the reflectivity maximum. This was demonstrated by Russel and Uthe (1975) with a great number of observations in the San Francisco bay area. We again confirmed it by comparing all reflectivity and potential temperature profiles which were available from this experiment.

In particular, we have studied the evolution of the mean horizontal wind in the convective layer continuously from sunrise to the time at which the inversion base rises above the sodar operating range (~300 m). The 20 min moving averaging results are presented every 5 min.

A typical example of our observations is shown in Fig. 3. The profiles are similar to those obtained in the Wangara experiment (Clarke *et al.*, 1971) and in the Minnesota experiment (Kaimal *et al.*, 1976). The following points are of particular interest:

- There are significant variations with height for both speed and direction below $0.3z_i$ (surface layer).
- Both speed and direction are essentially constant between 0.3 and $0.7z_i$ (well-mixed layer). In this area, we expect negligible mechanical turbulent ki-

netic energy modulation. This was confirmed by the studies of Caughey and Wyngaard (1979).

- The wind shear $d\bar{U}/dz$ has a maximum at approximately $z = z_i$. Both speed and reflectivity exhibit sharp changes at the inversion level.

Fig. 4 illustrates the nondimensional wind $\bar{U}k/u_*$, where k is the von Kármán constant, as a function of (z/z_i) for approximate universality for two cases. The two profiles are similar in shape but cannot be made to coincide. This suggests that the parameterization is inadequate and that an additional parameter must be introduced.

4. Law for the mean wind profile

In neutral conditions, the mean wind profile for the surface layer over homogeneous terrain can be written

$$\bar{U} = \frac{u_*}{k} \log \frac{z}{z_0}, \tag{2}$$

where z_0 is the surface roughness length. Thuillier and Lappe (1964) showed that Eq. (1) was valid above the surface layer in neutral air on the basis of observations on a 400 m tower. Tennekes (1973b) explained that Eq. (1) could only be used in a layer where z/z_0 is large enough $(z/z_0 \to \infty)$ and where the Coriolis force may be neglected $(zf/u_* \to 0)$. The range of validity of (1) has been called the "inertial sublayer" (Blackadar and Tennekes, 1968). Finally, Carl *et al.* (1973) showed that (2) was valid at least up to heights which are small compared to the depth of the PBL.

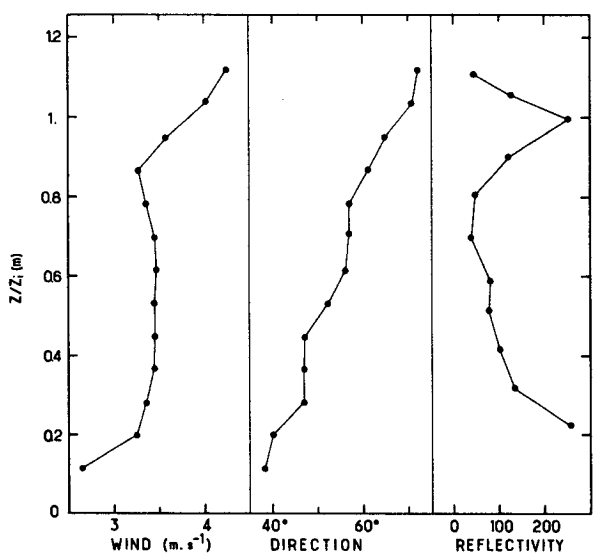

FIG. 3. A typical set of sodar observations obtained on 6 July at 0804 LT. The lowest inversion base was determined at a height of 175 m from both the reflectivity profile shown here and the potential temperature profile.

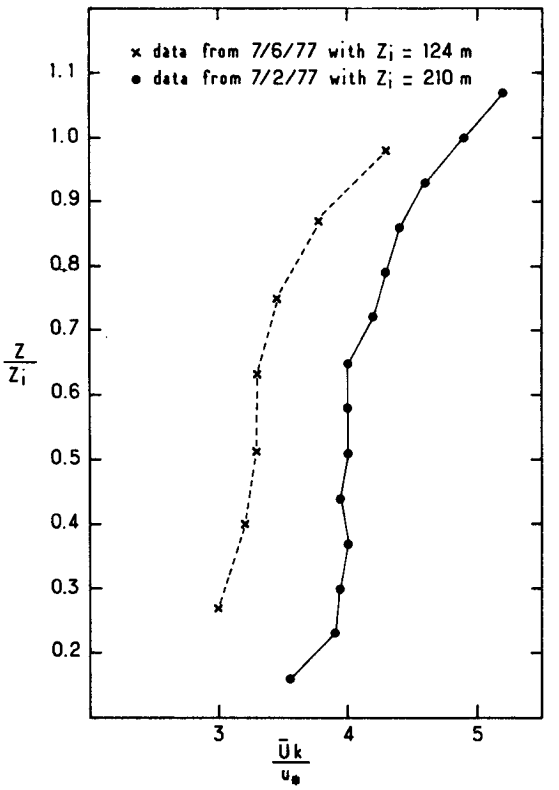

FIG. 4. Two non-dimensionalized mean horizontal wind profiles.

In unstable conditions, the nondimensional windshear

$$\phi = \frac{kz}{u_*} \frac{d\bar{U}}{dZ}, \tag{3}$$

obeys the following equations in the surface layer (Businger *et al.*, 1971):

$$\phi = \phi_1\left(\frac{z}{L}\right) = \left(1 - 15\frac{z}{L}\right)^{-1/4}, \quad L < 0. \tag{4}$$

Eq. (3) may be integrated to give an expression for the mean wind profile (Paulson, 1970), i.e.,

$$\bar{U} = \frac{u_*}{k}\left[\log \frac{z}{z_0} - \psi_1(z/L)\right], \tag{5}$$

where

$$\psi_1 = \int_{z_0}^{z} \frac{(1 - \phi_1)}{z}\, dz. \tag{6}$$

Formulas (3) and (4) are not valid above the surface layer.

From (5) and (6), we obtain

$$\left.\begin{aligned} \psi_1 &= 2\log[(1 + x)/2] + \log[(1 + x^2)/2] \\ &\quad - 2\tan^{-1}(x) + \pi/2 \\ x &= \phi_1^{-1} \end{aligned}\right\}. \tag{7}$$

Here we propose a formulation that will be valid for both the mixed and the surface layers. The height scales which are relevant for the mean horizontal wind profiles are L, z_i, and another length which results from integration of the wind shear. We first consider a nondimensional wind shear where L and z_i are the important height scales in the well-mixed and inversion layers. For this case we propose for the dimensionless wind shear an expression of the form

$$\phi = \phi_1(z/L) + \phi_2(z/z_i, z/L), \tag{8}$$

where the following conditions must be satisfied:

1) In the surface layer $\phi \approx \phi_1$.
2) In the well-mixed layer, around $z/z_i = 0.5$, $\phi \approx 0$.
3) Near $z/z_i = 1$, ϕ is maximum and this maximum is a function of z_i/L; it increases when z_i/L increases (Fig. 5).

From experimental values, we propose for ϕ an expression with a cosine whose value changes quickly near $z = z_i$, i.e.,

$$\left.\begin{aligned} \phi &= \phi_1 + (y - 8\phi_1)(z/z_i)^3 \\ y &= 4(1 + \cos 2\pi z/z_i) \end{aligned}\right\}. \tag{9}$$

Integration of Eq. (8) gives for the mean wind

$$\bar{U} = \frac{u_*}{k}\left(\log\frac{z}{z_0'} - \psi\right), \tag{10}$$

where

$$\psi = \psi_1 - 4I_2 + 8I_3,$$

with

$$I_2 = \frac{C^3}{3} + \frac{C}{2\pi^2}\cos 2\pi C + \left(\frac{C^2}{2\pi} - \frac{1}{4\pi^3}\sin 2\pi C\right),$$

$$I_3 = \frac{4}{b^3}\left(x^{11} - \frac{x^7}{3.5} + \frac{x^3}{3}\right),$$

$$C = z/z_i, \quad b = -\frac{15 z_i}{L}.$$

The empirical expression for $\bar{U}$ in the convective boundary layer enables us to determine u_*, L, z_0' and z_i on the basis of our observations. Note that it implies that the state of the ground surface can be felt on the horizontal wind up to heights of a few hundred meters. The subject is discussed further in the next section.

5. Systematic experimental confirmation

To assess the validity of our formulation, we have systematically compared its predictions to other independent observations. Using a simple computer program we have been able to fit our formula to the measured profiles and thus determine every 5 min the parameters u_*, L, z_i and z_0' from the 20 min moving average results. First, the values of u_* are compared to those derived from tower measurements and then the heat flux values obtained from L are compared to those obtained from the balance method.

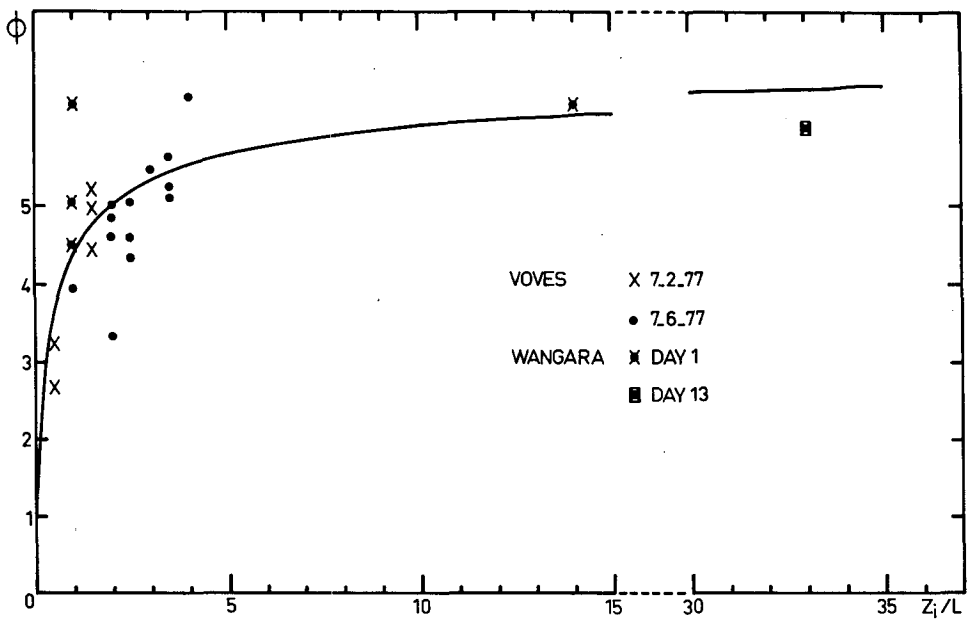

FIG. 5. The dimensionless wind shear as a function of z_i/L for $z/z_i = 1$.

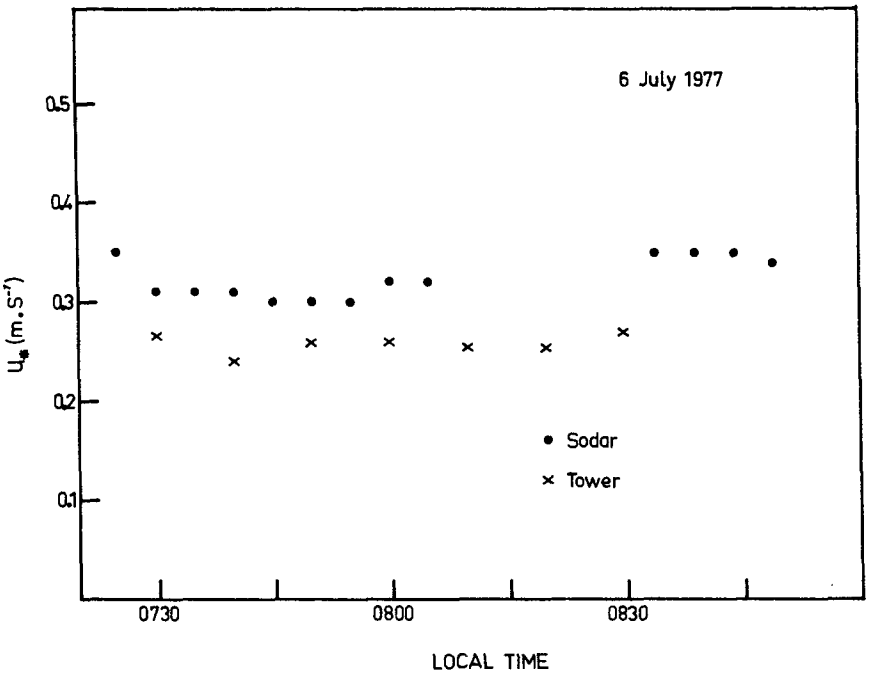

FIG. 6. Comparison of the friction velocity obtained with the sodar and with the tower.

a. The friction velocity

For the von Kármán constant, the value $k = 0.37$ was chosen. Fig. 6 shows a comparison between our sodar-derived values of u_* and the values obtained from tower measurements made by INRA for 6 July.

Although the difference in the two estimates is within the predicted error (on the order of 25%), the systematic difference appears significant. It implies that the spatially averaged surface stress over the area is greater than the local surface stress in the vicinity of the tower. This observation is hardly surprising when the region of Voves is considered as a whole. There are many heterogeneities in the ground surface, mostly associated with agricultural land use.

b. The sensible surface heat flux

From both u_* and L, the heat flux (W m^{-2}) is calculated (Table 2). It is rather difficult to draw a comparison between these fluxes and those from the balance method. [The averaging period for all data in Table 2 is 20 min, and 60 min for all data obtained with the balance method (Figs. 1a, 1b)]. The former are obtained at 5 min intervals and the latter at hour intervals. Our method lacks precision and the discrepancy between the two estimates is mainly due to the errors on u_* and L, but it has the advantage of showing the temporal sensible heat flux variability and could give an estimate of sensible heat flux in the absence of other measurements.

c. The length z'_0

The length z'_0 seems to be just a free parameter and we have to ask ourselves if it can be identified with a roughness length. Some large values for the roughness length were obtained recently by Schotz

TABLE 2. Voves parameters.

Day	Hour	z'_0 (m)	Z_i (m)	$-Z_i/L$	u_* (m s^{-1})	Surface heat flux (W m^{-2})
6 July 1977	0725	0.6	110	1	0.35	41
	0730	0.4	115	2	0.31	55
	0735	0.4	115	2	0.31	55
	0740	0.5	120	2	0.31	52
	0745	0.5	130	2.5	0.30	54
	0750	0.5	160	3.5	0.30	62
	0755	0.5	170	4	0.30	67
	0800	0.5	180	3.5	0.32	67
	0805	0.5	180	3.5	0.32	67
	0834	0.5	140	2.5	0.35	80
	0839	0.5	150	2	0.35	60
	0844	0.5	150	2.5	0.35	75
	0849	0.5	160	3	0.34	77
2 July 1977	0709	0.5	170	0.5	0.50	39
	0714	0.5	180	0.5	0.50	36
	0719	0.5	200	1	0.50	65
	0724	0.5	210	1	0.50	62
	0729	0.5	220	1	0.51	63
	0734	0.5	220	1.5	0.50	89
	0739	0.5	220	1.5	0.50	89
	0744	0.5	220	1.5	0.51	94

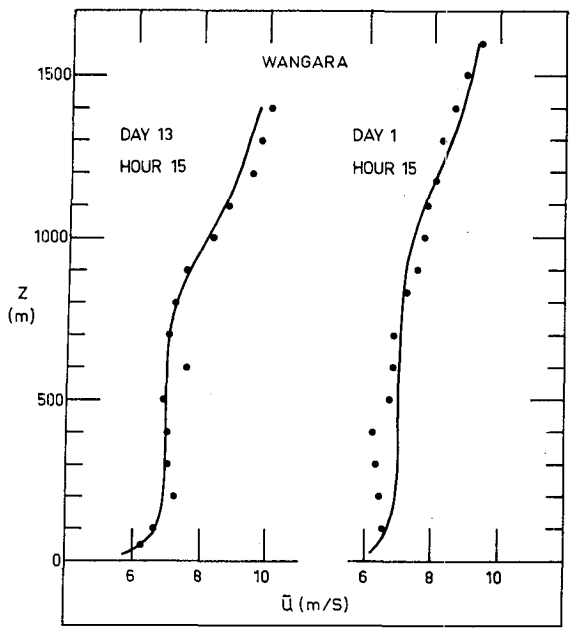

FIG. 7. Observed data points (Clarke *et al.*, 1971) and calculated wind speed profiles from present results.

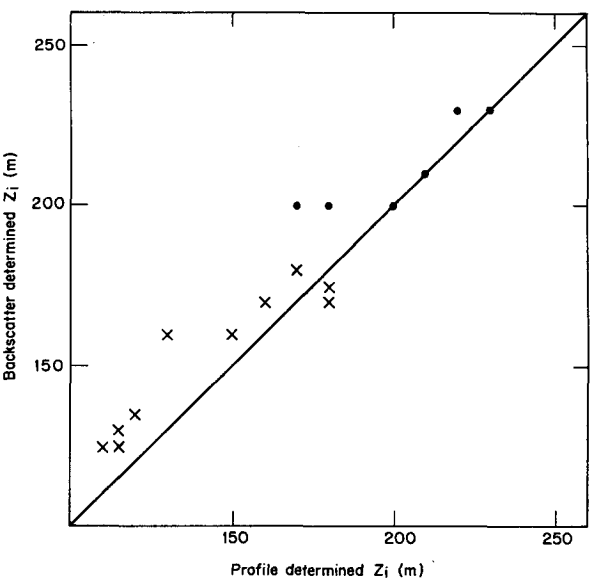

FIG. 8. Backscatter-determined z_i as a function of profile-determined z_i for 2 July 1977 (●) and 6 July 1977 (×).

and Panofsky (1980) who analyzed wind speeds from the Boulder Atmospheric Observatory 300 m tower. For west winds they estimate the roughness length z_0 at $\sim 0.04 \pm 0.02$ m, which are values generally obtained for similar terrain. But for south and southeast winds, the best estimate for the roughness length was ~ 0.25 m for the southern sector and 0.35 m for the southeastern. Schotz and Panofsky estimated that these values were much too large for the ground cover and call them the "effective" roughness lengths. An interesting conclusion is that over slightly rolling terrain, surface layer wind profile theory is still adequate provided that the true roughness length is replaced by a larger effective roughness length.

With a sodar, large volumes of air at great distances from each other are investigated so all the wind variations due to the terrain around the sounder are taken into account; thus the value $z_0' = 0.5 \pm 0.1$ m can be chosen for an "effective" mesoscale roughness length.

d. Wangara data

The Wangara data (Clarke *et al.*, 1971) represent an entirely independent set. One of the wind profiles chosen for study was taken as an example of an unstable case (day 13, hour 15), while the other one (day 1, hour 15) has a much smaller value of $-z_i/L$. In Fig. 7, calculated profiles have been obtained from Eq. (10). The value of L and z_i are those given by Melgarejo and Deardorff (1974). We found $z_0' = 0.02$ m and we corrected u_* to obtain a better fit (Table 3).

TABLE 3. Wangara parameters from Melgarejo and Deardorff (1974).

Day	Hour	Z_i (m)	u_* (m s^{-1})	L (m)	Corrected values for Fig. 8
1	15	1150	0.24	−80	$u_* = 0.27$ m s^{-1}
13	15	950	0.27	−28	$u_* = 0.29$ m s^{-1}

e. The inversion base height z_i

The height z_i can be defined from wind observations; as noted earlier it coincides with the height of the maximum backscattered acoustic intensity. A comparison between values of z_i determined from profiles and from backscatter observations is given in Fig. 8. The backscatter determined values are generally higher than the profile values—the difference is about 15 m, a distance equivalent to one gate.

6. Conclusions

We have shown that the dimensionless wind shear in the convective boundary layer follows a simple pattern which is best expressed in terms of z/z_i and z/L. The value of the wind shear at the inversion increases with z_i/L.

An expression for the mean horizontal wind profile was developed which is consistent with convective layer similarity laws and with matching in the surface layer. It is in good agreement with both sodar and tower measurements for the different days investigated and gives useful insight into mean horizontal wind parametrization. It shows that z_i, u_* and L can be determined with reasonable accuracy from

horizontal wind profiles in the convective boundary layer.

Acknowledgments. This work was supported by the Action Thématique Programmée, Recherches Atmospheriques of the Institut National d'Astrophysique et de Geophysique, by the Centre National de la Recherche Scientifique and by the Centre National d'Etudes des Télécommunications. The authors wish to acknowledge the help of all the technical staff from the various scientific organisations involved (Centre de Recherches en Physique de l'Environnement, Institut National de Recherches Agronomiques, Etablissement d'Etudes et de Recherches Météorologiques) who made the data collection possible. The useful suggestions and criticisms made by Prof. Hans A. Panofsky and Prof. Denis W. Thomson during a careful review of the paper are also gratefully acknowledged.

REFERENCES

Alavi, A. S., and G. M. Jenkins, 1965: An example of digital filtering. *Appl. Statist.*, **14,** 70–83.

Andre, J. C., G. De Moor, P. Lacarrere, G. Therry and R. Du Vachat, 1978: Modeling the 24-hour evolution of the mean and turbulent structures of the planetary boundary layer. *J. Atmos. Sci.*, **10,** 1861–1883.

Artaz, M. A., and J. C. Andre, 1980: Similarity studies of entrainment in convective mixed layers. *Bound.-Layer Meteor.*, **19,** 51–66.

Aubry, M., R. Chezlemas and A. Spizzichino, 1974: Preliminary results of the atmospheric sounding program at CNET. *Bound.-Layer Meteor.*, **7,** 513–519.

Blackadar, A. D., and H. Tennekes, 1968: Asymptotic similarity in neutral barotropic planetary boundary layers. *J. Atmos. Sci.*, **25,** 1015–1020.

Bouteloup, P., 1979: Interactions entre thermiques et ondes de gravité. Diplôme d'Etudes Approfondies, Paris, 65 pp.

Businger, J. A., J. C. Wyngaard, Y. Izumi and E. F. Bradley, 1971: Flux profile relationships in the atmospheric surface layer. *J. Atmos. Sci.*, **28,** 181–189.

Carl, D. M., T. C. Tarbell and H. A. Panofsky, 1973: Profiles of wind and temperature from towers over homogeneous terrain. *J. Atmos. Sci.*, **30,** 788–794.

Caughey, S. J., and J. C. Kaimal, 1977: Vertical heat flux in the convective boundary layer. *Quart. J. Roy. Meteor. Soc.*, **103,** 811–815.

——, and J. C. Wyngaard, 1979: The turbulence kinetic energy budget in convective conditions. *Quart. J. Roy. Meteor. Soc.*, **105,** 213–239.

Clarke, R. W., A. J. Dyer, R. R. Brook, O. G. Reid and A. J. Troup, 1971: The Wangara experiment, boundary layer data. Paper No. 19, Division Meteorological Physics, CSIRO, Australia, 362 pp.

Deardorff, J. W., 1974: Three-dimensional numerical study of the height and mean structure of a heated planetary boundary layer. *Bound.-Layer Meteor.*, **7,** 81–106.

——, 1979: Prediction of convective mixed-layer entrainment for realistic capping inversion structure. *J. Atmos. Sci.*, **36,** 424–436.

Dubosclard, G., 1980: Comparison between observed and predicted values for the entrainment coefficient in the planetary boundary layer. *Bound.-Layer Meteor.*, **18,** 473–483.

Kaimal, J. C., J. C. Wyngaard, D. A. Haugen, O. R. Coté, Y. Izumi, S. J. Caughey and C. J. Readings, 1976: Turbulence structure in the convective boundary layer. *J. Atmos. Sci.*, **33,** 2152–2169.

Melgarejo, J. W., and J. W. Deardorff, 1974: Stability functions for the boundary layer laws based upon observed boundary layer heights. *J. Atmos. Sci.*, **31,** 1324–1333.

Paulson, C. A., 1970: The mathematical representation of wind speed and temperature profiles in the unstable surface layer. *J. Appl. Meteor.*, **9,** 857–861.

Perrier, A., B. Itier, J. M. Bertolini and N. B. Katerji, 1976: A new device for continuous recording of energy balance of natural surfaces. *Agric. Meteor.*, **16,** 71–84.

Pielke, R. A., and Y. Mahrer, 1975: Representation of the heated planetary boundary layer in mesoscale models with coarse vertical resolution. *J. Atmos. Sci.*, **12,** 2288–2308.

Russel, B. P., and E. E. Uthe, 1975: Development of an acoustic sounder network for air pollution and land use applications. *Third Workshop in Atmospheric Acoustics*, Toronto, 45 pp.

Schotz, S., and H. A. Panofsky, 1980: Wind characteristics at the Boulder atmospheric observatory. *Bound.-Layer Meteor.*, **19,** 155–164.

Stull, R. B., 1976: The energetics of entrainment across a density interface. *J. Atmos. Sci.*, **33,** 1260–1267.

Tennekes, H., 1973a: A model for the dynamics of the inversion above a convective boundary layer. *J. Atmos. Sci.*, **30,** 558–567.

Tennekes, H., 1973b: The logarithmic wind profile. *J. Atmos. Sci.*, **30,** 234–238.

Thuillier, R. H., and V. O. Lappe, 1964: Wind and temperature profile characteristics from observations on a 1400 ft tower. *J. Appl. Meteor.*, **9,** 857–861.

Weill, A., F. Baudin, J. P. Goutorbe, P. Van Grunderbeeck and P. Leberre, 1978: Turbulence structure in temperature inversions and in convective fields as observed by doppler sodar. *Bound.-Layer Meteor.*, **15,** 375–390.

Wyngaard, J. C., and O. R. Coté, 1974: The evolution of a convective planetary boundary layer. A higher-order-closure model study. *Bound.-Layer Meteor.*, **7,** 289–304.

Zeman, O., and J. L. Lumley, 1976: Modeling buoyancy driven mixed layers. *J. Atmos. Sci.*, **10,** 1974–1988.

Zilitinkevich, S. S., and J. W. Deardorff, 1974: Similarity theory for the planetary boundary layer of time dependent height. *J. Atmos. Sci.*, **31,** 1449–1452.